

Reply to "Comment on 'Statistical Features of Short-Period and Long-Period Near-Source Ground Motions' by Masumi Yamada, Anna H. Olsen, and Thomas H. Heaton" by Roberto Paolucci, Carlo Cauzzi, Ezio Faccioli, Marco Stupazzini, and Manuela Villani

By Masumi Yamada, Anna H. Olsen, and Thomas H. Heaton

The comment by Paolucci and colleagues (Paolucci et al. 2011) states that a probabilistic seismic hazard analysis (PSHA) can provide “reliable prediction of long-period spectral ordinates.” The result of such an analysis would be in contrast to the more uncertain prediction suggested by our empirical, and proposed theoretical, distribution of near-source ground displacements in past, large magnitude earthquakes (Yamada et al., 2009). After addressing two specific concerns of Paolucci and colleagues, we use the balance of this reply to discuss the apparent differences between a PSHA and our observations. These two approaches to understanding the seismic hazard of long-period ground motions —past observations and PSHAs— should be consistent, even though they view the problem from different perspectives.

Paolucci and colleagues prefer to use elastic spectral displacement as the intensity measure of long-period ground motions rather than peak ground displacement (PGD). Spectral displacement and PGD, however, are highly correlated. We calculate the elastic spectral displacements ( $S_d$ ) of our original set of recorded ground motions. We first find  $S_d$  for each horizontal component over a range of periods from 3 to 9 s at a 0.02 s interval, with damping at 5% of critical. At each period, we take the square root of the sum of the maximum squared  $S_d$  of each component. Then we find the geometric mean over three ranges of periods: 3-5, 5-7, and 7-9 s. We average the spectral displacements in each range to find a more stable measure of the long-period spectrum. We also calculate pseudo- $S_d$  from the spectral accelerations ( $S_a$ ) reported in the current Next Generation Attenuation database (see Data and Resources Section).<sup>1</sup> Figure 1 shows that the logarithms of PGD and  $S_d$  are highly correlated, with correlation coefficients of 0.9405 (3-5 s), 0.9707 (5-7 s), and 0.9750 (7-9 s) for the records collected in Yamada et al. (2009). Also, we find similar correlations of PGD and pseudo- $S_d$  from the NGA database. We prefer to use PGD because it is period independent, physically intuitive, and more concise than a family of spectral curves. Although the value of PGD is certainly sensitive to the processing of a recorded ground motion, our conclusions do not depend on particular values of PGD.

In our original paper, we showed the distributions of peak ground acceleration (PGA) and PGD from near-source sites (that is, within 10 km of the surface

---

<sup>1</sup> The NGA project chose to employ the GMRotI50 algorithm (Boore et al., 2006) to combine horizontal components of ground motion. The NGA  $S_a$  are reported at fewer periods than we calculate within the three ranges. Within each range of periods, we find the geometric mean of the pseudo- $S_d$  at the periods given in the NGA database.

projection of the rupture, also known as a Joyner-Boore distance less than 10 km) of large magnitude (between 6.5 and 8) earthquakes recorded in the years 1979 through 2004.<sup>2</sup> We now add near-source records from similar sites since 2004 (Table 1), and Figures 2 and 3 update the PGA and PGD distributions, respectively, with these records. Our updated PGA and PGD distributions are consistent with the distributions presented in Yamada et al. (2009). In the years 2005 through 2009, there was no well-recorded large earthquake. Thus, we would not expect our observed distribution of PGD to change significantly. Figures 2 and 3 also overlay PGAs and PGDs from the near-source of past events with magnitudes greater than or equal to 6.5 as reported in the current Next Generation Attenuation database (see Data and Resources Section). The NGA distributions are consistent with our empirical distributions.

Furthermore, we perform statistical tests on the empirical distributions of PGA and PGD to determine whether they are consistent with log-normal or log-uniform distributions. We apply Lilliefors tests of the null hypothesis that each observed PGA dataset is drawn from a log-normal population distribution (Lilliefors, 1967). The null hypothesis cannot be rejected for the three PGA datasets (YOH2009: p-value = 0.4617; YOH2009 updated: p-value = 0.8070; PEER NGA: p-value = 0.3236); these observed PGAs could have been drawn from a log-normal population distribution. We apply Chi-square tests of the null hypothesis that each PGD dataset is drawn from a truncated, uniform population distribution on a logarithmic scale (see, for example, Devore (2000) Section 14.1). We limit the range of the log-uniform distribution because we select records on a limited range of magnitudes. These distributions,  $p_{\text{uniform}}$ , are defined as:

$$p_{\text{uniform}} = \begin{cases} 1, & -1.65 \leq \log_{10}(\text{PGD}) \leq -0.05 \\ 0, & \text{otherwise} \end{cases}$$

for our original and updated empirical distributions; and

$$p_{\text{uniform}} = \begin{cases} 1, & -1.35 \leq \log_{10}(\text{PGD}) \leq -0.15 \\ 0, & \text{otherwise} \end{cases}$$

for the NGA distribution of PGD. The null hypothesis cannot be rejected for the three PGD datasets (YOH2009: p-value = 0.2630; YOH2009 updated: p-value = 0.2405; PEER NGA: p-value = 0.0799); these observations could have been drawn from a truncated, log-uniform population distribution. To be clear, these statistical tests do not demonstrate that the population distributions of PGA and PGD in the near-

---

<sup>2</sup> In our original paper we incorrectly stated the algorithm we use to calculate PGA (or PGD) for the recorded ground motions. We calculate a peak ground measure by first finding the maximum squared acceleration (displacement) for each horizontal component time history. The PGA (PGD) is the square root of the sum of the squared maxima.

source of large earthquake are log-normal and log-uniform, respectively. Rather, the available observations are consistent with these population distributions.

There is no question that seismic hazards exist throughout the world. However the question of how to conceptualize and quantify these hazards remains. How do we as a seismological and earthquake engineering community understand the likelihood and intensity of future ground motions? There should be several, distinct approaches to quantifying seismic hazard, because, if the approaches provide consistent results, the community can have greater confidence in our understanding of seismic hazard. If these various approaches provide inconsistent results, then we must identify the source of the inconsistencies and work to improve our understanding.

Returning to the present discussion of future long-period ground motions, we seek to determine whether different techniques of quantifying this seismic hazard are consistent. We begin with an example from recent work of the Tall Buildings Initiative of the Pacific Earthquake Engineering Research Center (PEER). Their study analyzes the performance—both structural and economic—of forty- or forty-two-story buildings designed according to three procedures (PEER, 2010). To this end, the researchers use five sets of fifteen ground motions to represent five levels of seismic hazard for a site in downtown Los Angeles (see Data and Resources Section). The hazard levels are defined by return periods of 4,975, 2,475 (the maximum considered earthquake, MCE), 475 (the design basis earthquake, DBE), 43, and 25 years. The ground motions representing these hazard levels result from selecting recorded or simulated ground motions and then scaling them according to the technique of spectrum matching (Jones and Zareian, 2010). Figure 3 shows the PGDs that represent the 4,975- and 2,475-year hazard levels compared with the empirical distributions of near-source displacements. According to the Tall Buildings Initiative, the 4,975-year hazard level represents “extremely rare shaking ... which is well beyond the ground motion level generally considered in the building industry” (PEER, 2010). However, when we compare the PGDs representing the 4,975- and 2,475-year hazards to our set of observed PGDs, these “rare” ground motions are smaller than the largest recorded observations. In fact, the geometric mean PGD within the 4,975-year hazard level (1.00 m) is much smaller than the most extreme observed PGD (2.99 m). Given the considerable number of identified faults with the capacity to generate large earthquakes—and an unknown number of unidentified faults—in the Los Angeles basin and proximate areas (Dolan et al., 1995), why are 1-in-4,975-year ground motions for a site in downtown Los Angeles no larger than worldwide observations from the last thirty years?

We can also compare the PGDs of the ground motions representing the seismic hazard at a site in downtown Los Angeles to the PGDs of simulated ground motions resulting from hypothetical ruptures of the Puente Hills fault system. This fault system underlies downtown Los Angeles and the areas immediately east, and it has generated at least four large, blind thrust earthquakes in the past 11,000 years (Dolan et al., 2003). Converting this observation to a recurrence interval suggests

that the Puente Hills fault system generates a magnitude 7.2 to 7.5 earthquake with an average recurrence of 2,800 years. Graves and Somerville (2005) simulated broadband ground motions throughout the Los Angeles basin from a hypothetical M 7.15 rupture of this fault (see Data and Resources Section). Figure 3 compares the PGDs at 648 sites for five scenario ruptures with the PGDs of the PSHA described above. The Graves and Somerville simulations of a roughly 2,800-year event produce numerous PGDs in excess of the PGDs representing the 4,975-year hazard level. Granted, the hazard analysis is site-specific, and the Graves and Somerville ground motions are for sites throughout the Los Angeles basin. However, is our knowledge of future ground motions at sites in downtown Los Angeles so certain that it precludes the possibility of displacements at least as large as the largest displacements in these simulations?

Accurately characterizing the hazard of long period ground motions is important for assessing the performance of long period structures and, in particular, for designing tall buildings in areas of high seismicity. In a recent study, Jones and Zareian (2010) applied the seventy-five, spectrum matched ground motions just mentioned to forty-story building models of a buckling-restrained braced frame, designed according to three procedures: the 2006 International Building Code (abbreviated CBD, following Jones and Zareian); the Los Angeles Tall Buildings Structural Design Council Alternative Procedures for Tall Buildings (PBD); and the PEER Tall Buildings Initiative Guidelines (PBD+). Jones and Zareian found that one of the 2,475-year hazard ground motions caused an inter-story drift ratio (IDR) greater than 3%—which they deem the collapse prevention limit—in the PBD building model. For the same building, three of the 4,975-year hazard ground motions induced responses in excess of this limit. For the CBD building model, one 4,975-year hazard ground motion induced a response greater than this limit. None of the 2,475- or 4,975-year hazard ground motions caused the PBD+ building model to exceed the collapse prevention limit. We assume that the ground motions causing the largest building responses have the largest PGDs within each hazard level. Therefore, ground motions with PGDs of roughly 1.3 m or greater can cause forty-story building models of buckling-restrained braced frames, designed with current techniques, to develop IDRs larger than 3%, the value associated with collapse prevention.

Jones and Zareian (2010) also applied two sets of nine near-fault ground motions from the Graves and Somerville (2005) Puente Hills simulations. Of these eighteen ground motions: 28% caused the CBD model to exceed the collapse prevention limit; 33% caused the PBD model to exceed this limit; and 50% caused the PBD+ model to exceed this limit. Certainly, non-linear time history analyses of forty-story buildings with different lateral force-resisting systems—or analyses of tall buildings with more or fewer stories—will find different cutoffs for ground motions that cause buildings to exceed their collapse prevention limits. Nonetheless, PGDs of 1-2 m should be of concern when assessing tall buildings. A recent PSHA for a site in downtown Los Angeles at this level of ground displacement seems to be inconsistent with the past thirty years of recorded ground motions and inconsistent

with realistic simulations of ruptures on a well-studied fault system. If these hazard assessments are too low, then the calculated probabilities of unsafe building responses are also too low.

There are well-known concerns with each model of a PSHA (that is, the definition of the earthquake sources, magnitude-frequency relationships, and ground motion prediction equations). Quantifying the uncertainties associated with each model is robust for near-source short-period ground motions because there is sufficient available data from past events to establish that the distribution is approximately log-normal and independent of the fault slip. Data on near-source long-period ground motions from large-slip earthquakes are not so readily available, although the occurrence of just a small number of large urban earthquakes could dramatically change that.

Estimating the probability of near-source shaking is further complicated by the fact that there are numerous examples of very damaging earthquakes caused by either unknown or low slip-rate faults. For example, the 1994 Northridge ( $M_w$  6.7) and 2008 Iwate-Miyagi Nairiku ( $M_w$  6.9; Toda et al., 2010) earthquakes ruptured previously unidentified faults. In a seismically active region, not identifying a fault has less severe consequences for short-period ground motion prediction as compared to long-period. Since PGA saturates with magnitude, identifying a “new” fault would not significantly change the expectation of a reasonably large PGA. If a major fault is not included in a PSHA, there may be an unaccounted potential for a larger PGD than otherwise expected.

Second, magnitude-frequency relationships are not well-constrained at large magnitudes because of the paucity of data. A PSHA might extrapolate the Gutenberg-Richter relationship from frequent events, or place an upper bound on this relationship, or define a characteristic earthquake (Kramer, 1996, Section 4.4.1.2). These various approaches reflect our incomplete knowledge of the recurrence of large earthquakes. Propagating this uncertainty to the prediction of future ground motions should result in greater uncertainties for long-period—but not necessarily for short-period—ground motions. Further, there have been observations of large slips (and thus large magnitudes) in areas previously believed to have only a moderate seismic hazard. The 1976 earthquake in Tangshan, China (Allen et al., 1984) and the 1995 Kobe earthquake on Awaji Island (Toda et al., 1996) are examples of this.

Third, there is not a lot of data to define robust ground motion prediction equations in the near-source of large earthquakes. We collect 174 near-source records from past large earthquakes (146 in Yamada et al. (2009) and 28 additional records here). In the current Next Generation Attenuation database there are 129 such records, accounting for only 3.6% of the total database. Ground motion prediction equations rely on the character of empirical data from larger distances and smaller magnitudes to inform the predictions of ground motions in the near-source of large magnitude earthquakes. These assumptions may not be consistent with scaling

relations for fault slip derived from teleseismic observations of many large earthquakes.

Not only are the large uncertainties in future long-period ground motions the result of a relatively short instrumental record, these large uncertainties result from our limited theoretical knowledge of earthquake sources. As shown in our original paper, magnitude and PGD are correlated in the near source (also see Aagaard and Heaton, 2004). However, the physical quantity measured by magnitude is the product of crustal rigidity, the rupture area, and the average slip. If we seek a predictive theory for PGD in the near source, we must anticipate the distribution of slip on a fault (and thus average slip) and anticipate the rupture area. Compilations of source models (for example, the Finite-Source Rupture Model Database (Mai 2010)) demonstrate that slip can have a considerable spatial variability and that slip is difficult to reliably estimate, as evidenced by many plausible slip distributions inferred from the same past event. Theories of slip initiation and termination are still open to debate, thus making any theoretical prediction of rupture area quite uncertain. We believe the best current “theory” applicable to the prediction of PGD in the near-source are the scaling relations we employed in our original paper.

At present, predictions of future long-period ground motions from probabilistic seismic hazard analyses appear inconsistent with—specifically, smaller than—past observations and plausible rupture simulations. Perhaps current PSHAs do not properly account for the inherent uncertainties in predicting near-source ground displacements. These uncertainties exist because near-source ground displacements at the surface are strongly correlated with the amplitude of slip on nearby patches of fault rupture, and anticipating fault slip is highly uncertain given our current knowledge. Until we have enough data or a reliable theory, any prediction of long-period ground motion in the near-source of large earthquakes will remain highly uncertain.

## Data and Resources

The Pacific Earthquake Engineering Research Center’s Next Generation Attenuation database flatfile can be downloaded at <http://peer.berkeley.edu/nga/>. We use public version 7.3 in this work (accessed 12 June 2010). The strong motion data for the 2007 Noto-hanto, 2007 Chuetsu-oki, 2008 Iwate-Miyagi Nairiku, and 2009 Suruga-wan earthquakes were recorded by the K-NET and KiK-net seismic networks, operated by the National Research Institute for Earth Science and Disaster Prevention in Japan ([www.kyoshin.bosai.go.jp](http://www.kyoshin.bosai.go.jp); last accessed September 2010). The dataset of the 2008 Wenchuan earthquake was recorded by the National Strong Motion Observation Network System of China, managed by the National Strong Motion Observation Center and local strong motion observation centers ([www.csmnc.net/selnewxjx1.asp?id=749](http://www.csmnc.net/selnewxjx1.asp?id=749); last accessed September 2010).

Farzin Zareian, in personal communication of June 2010, provided the seventy-five ground motions used in the PEER study of downtown Los Angeles. In a personal communication of March 2007, Robert Graves provided the ground motion time histories described in Graves and Somerville (2005).

#### References:

- Aagaard, B. and T. Heaton (2004). Near-source ground motions from simulations of sustained intersonic and supersonic fault ruptures, *Bull. Seismol. Soc. Am.* 94, no.6, 2064-2078.
- Allen, C. R., A. R. Gillespie, HAN Yuan, K. E. Sieh, ZHANG Buchun, and ZHU Chengnan (1984, June) Red River and associated faults, Yunnan Province, China: Quaternary geology, slip rates, and seismic hazard, *Geological Society of America Bulletin* 95, 686-700.
- Aoi, S., B. Enescu, W. Suzuki, Y. Asano, K. Obara, T. Kunugi, and K. Shiomi (2010). Stress transfer in the Tokai subduction zone from the 2009 Suruga Bay earthquake in Japan, *Nature Geoscience*, 3, 496-500.
- Aoi, S., H. Sekiguchi, N. Morikawa, and T. Kunugi (2008). Source process of the 2007 Niigata-ken Chuetsu-oki earthquake derived from near-fault strong motion data, *Earth, planets and space* 60, no.11, 1131-1135.
- Boore, D., J. Watson-Lamprey, N. Abrahamson (2006) Orientation-independent measures of ground motion, *Bull. Seismol. Soc. Am.* 96, no.4A, 1502-1511.
- Devore, Jay L. (2000) Probability and Statistics for Engineering and the Sciences. 5<sup>th</sup> ed. Pacific Grove, CA: Duxbury.
- Dolan, J., K. Sieh, T. Rockwell, R. Yeats, J. Shaw, J. Suppe, G. Huftile, and E. Gath (1995). Prospects for larger or more frequent earthquakes in the Los Angeles metropolitan region, *Science* 267, no.5195, 199-205.
- Dolan, J., S. Christofferson, J. Shaw (2003). Recognition of paleoearthquakes on the Puente Hills blind thrust fault, California, *Science* 300, no.5616, 115-118.
- Graves, R. and P. Somerville (2005). Broadband ground motion simulations for scenario ruptures of the Puente Hills fault, *Proceedings of the 8th National Conference on Earthquake Engineering*, San Francisco, California, USA, paper no. 1052.
- Jones, P. and F. Zareian (2010). Seismic response of a forty-story buckling restrained braced frame designed for the Los Angeles region, Proceedings of the 2010 Annual Meeting of the Los Angeles Tall Building Design Council, May, 2010, Los Angeles, CA, 86-93.

- Koketsu, K., Y. Yokota, H. Ghasemi, K. Hikima, H. Miyake, and Z. Wang (2010). Source process and ground motions of the 2008 Wenchuan Earthquake. In "Investigation report of the May 12th 2008, Wenchuan earthquake, China, Grant-in-Aid for Special Purposes of 2008, Ministry of Education, Culture, Sports, Science and Technology (MEXT). No. 20900002." <http://shake.iis.u-tokyo.ac.jp/wenchuan/>
- Kramer, Steven L. (1996) Geotechnical Earthquake Engineering. Upper Saddle River, New Jersey: Prentice Hall.
- Kurahashi, S., K. Masaki, and K. Irikura (2008). Source model of the 2007 Noto-Hanto earthquake (Mw 6.7) for estimating broad-band strong ground motion. *Earth, planets and space* 60, no.2, 89-94.
- Lilliefors, Hubert. W. (1967) On the Kolmogorov-Smirnov Test for Normality with Mean and Variance Unknown, *Journal of the American Statistical Association* 62, no. 318, 399-402.
- Mai, P. M. (2010). Finite-Source Rupture Model Database (SRCMOD). <http://www.seismo.ethz.ch/srcmod/Homepage.html>. Accessed 2 July 2010.
- Paolucci, R., C. Cauzzi, E. Faccioli, M. Stupazzini, and M. Villani (2011). Comment on "Statistical features of short-period and long-period near-source ground motions" by Masumi Yamada, Anna H. Olsen, and Thomas H. Heaton, *Bull. Seismol. Soc. Am.*
- PEER (2010) Implications of performance-based seismic design of tall buildings, Proceedings of the 2010 Annual Meeting of the Los Angeles Tall Building Design Council, May, 2010, Los Angeles, CA, 1-2.
- Suzuki, W., S. Aoi, and H. Sekiguchi (2010). Rupture Process of the 2008 Iwate-Miyagi Nairiku, Japan, Earthquake Derived from Near-Source Strong-Motion Records, *Bull. Seismol. Soc. Am.* 100, no.1 , 256-266.
- Toda S., T Maruyama, M. Yoshimi, H. Kaneda, Y. Awata, T. Yoshioka, and R. Ando (2010). Surface rupture associated with the 2008 Iwate-Miyagi Nairiku, Japan, earthquake and its implications to the rupture process and evaluation of active faults, *Zisin : Journal of the Seismological Society of Japan* 62, no.4, 153-178 (in Japanese with English abstract).
- Toda, Shinji, Ryuta Hataya, Shintaro Abe, and Katsuyoshi Miyakoshi (1996). The 1995 Kobe earthquake and problems of evaluation of active faults in Japan. *Engineering Geology* 43, 151-167.
- Yamada, M., A. Olsen, and T. Heaton (2009) Statistical Features of Short- and Long-Period Near-Source Ground Motions, *Bull. Seismol. Soc. Am.* 99, no.6, 3264-3274.



Tables:

**Table 1. Earthquakes since 2004 that provided near-source records from large earthquakes. \***

<i>Earthquake</i>	$M_w$ <sup>†</sup>	<i>N</i>	<i>Focal Depth</i> <sup>†</sup>	<i>Fault Model</i>
2007 Noto-hanto	6.7	3	8.0	Kurahashi et al. 2008
2007 Chuetsu-oki	6.6	10	12.0	Aoi et al. 2008
2008 Wenchuan	7.9	6	19.0	Koketsu et al. 2010
2008 Iwate-Miyagi Nairiku	6.9	7	7.8	Suzuki et al. 2010
2009 Suruga-wan	6.4	2	26.8	Aoi et al. 2010

\* Near-source records are within 10 km of the surface projection of the rupture; large earthquakes are those with magnitudes greater than or equal to 6.4.

<sup>†</sup> The magnitude and focal depth for the Suruga-wan earthquake is from the United States Geological Survey; the magnitudes and focal depths for all other earthquakes are from the Harvard CMT model. This table augments table 1 in Yamada et al. (2009). (See the Data and Resources Section for descriptions of the data sources.)

Figure captions:

**Figure 1. Peak ground displacement (PGD) versus spectral displacement ( $S_d$ ) for three ranges of long-period ( $T$ ):  $T = 3-5$  s (left);  $T = 5-7$  s (middle); and  $T = 7-9$  s (right). Circles represent data from the NGA database, and crosses represent data from Yamada et al. (2009). For periods of 3-5s, the slope of PGD versus  $S_d$  is closest to one. For periods of 7-9 s, the correlation coefficient,  $R$ , between the logarithms of PGD and  $S_d$  is largest.**

**Figure 2. Distributions of recorded peak ground accelerations (PGA). The YOH2009 distribution was published in Yamada et al. (2009). The “YOH2009 updated” distribution adds records since 2004 to the original distribution. The PEER NGA distribution uses data from the current NGA database. The three PGA distributions are consistent with a log-normal distribution. There has been no well-recorded large earthquake since 2004, which we expect would change the PGD distribution in Figure 3 but not the PGA distributions here.**

**Figure 3. Distributions of recorded peak ground displacement (PGD) at top and box-and-whisker plots for sites in the Los Angeles area at bottom. The “YOH2009,” “YOH2009 updated,” and “PEER NGA”**

distributions represent the same datasets described in the caption for Figure 2. The three PGD distributions at the top of this figure are consistent with a truncated log-uniform distribution. In the bottom plot, we locate the quartiles of three additional datasets. A probabilistic seismic hazard analysis for a site in downtown Los Angeles used fifteen ground motions to represent the 4,975-year hazard and an additional fifteen motions to represent the 2,475-year hazard. Graves and Somerville (2005) simulated five M 7.15 ruptures on the Puente Hills fault system and generated ground motions at 648 sites in the Los Angeles region (

Figures:

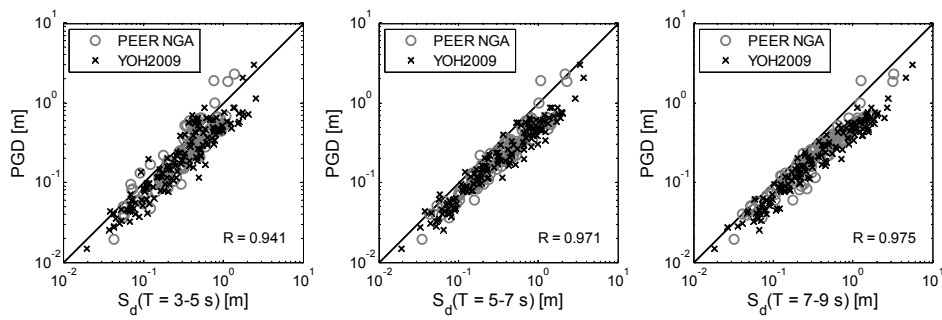


Figure 1

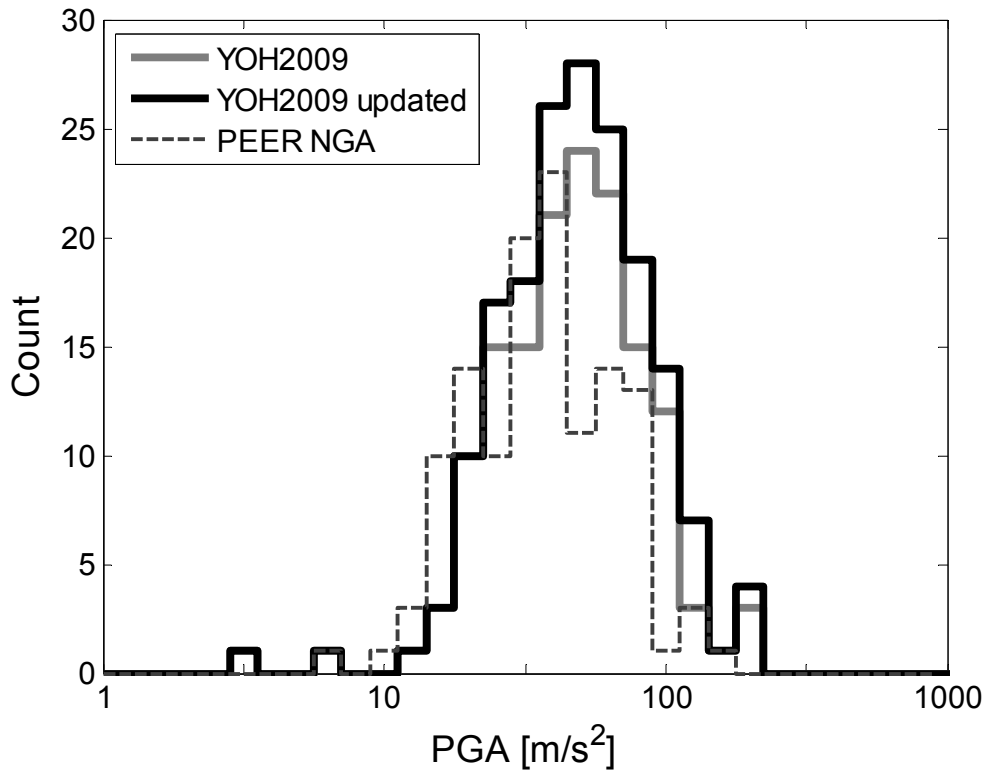


Figure 2

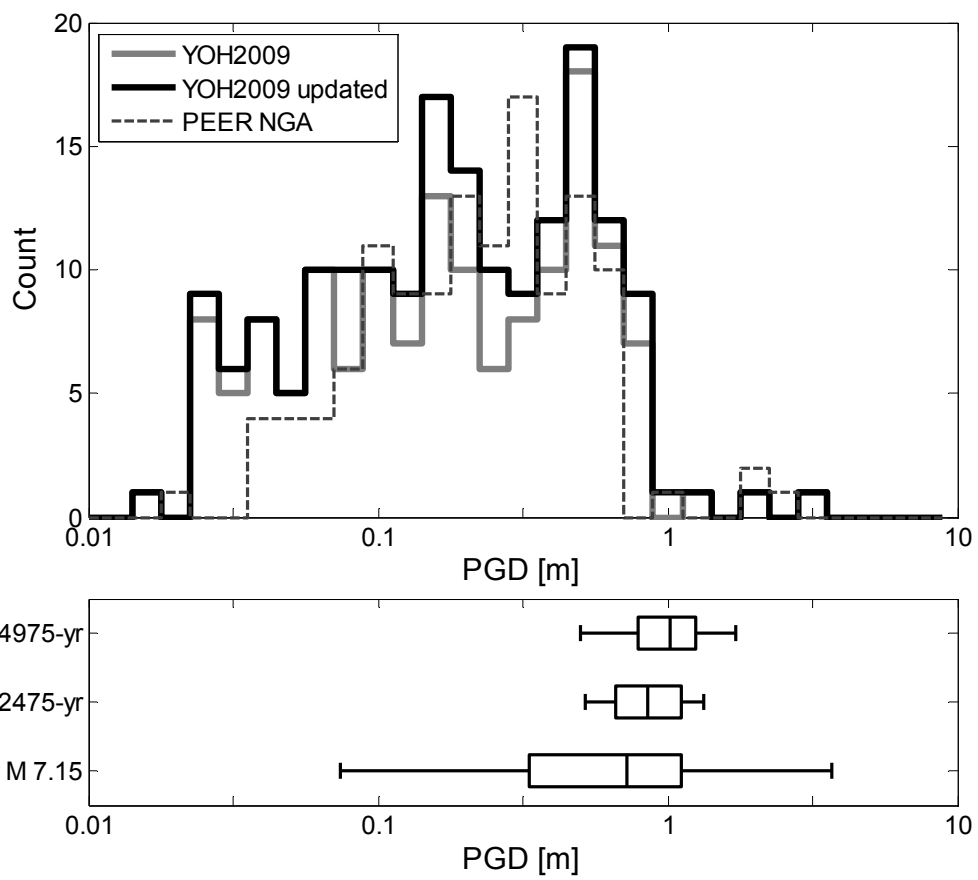


Figure 3